Thin aluminum/polyimide optical blocking filter study for the Lynx x-ray mission

Benjamin R. Zeiger[*a], Charles Tarrio[b], Travis Ayers[a]
[a]Luxel Corporation, PO Box 1879, Friday Harbor, WA, USA 98250-1841; [b]Sensor Science Division, National Institute of Standards and Technology, Gaithersburg, MD, USA, 20899-8411

ABSTRACT

The Lynx x-ray mission will push thin film filters to larger apertures and thinner profiles than those of any preceding mission. We present a study of the uniformity of deposition with existing technology and the consequences of oxidation on 10-15 nm thick Al films on LUXFilm®† polyimide. We present visible and infrared transmission measurements of thin aluminum filters and the results of a photon-driven oxidation study at the Beamline 1 of the Synchrotron Ultraviolet Radiation Facility at the National Institute of Standards and Technology. We conclude that, from a deposition and oxidation standpoint, Al optical blocking layers at this thickness are viable.

Keywords: microcalorimeter, thin film deposition, filter, optical blocking filters, Lynx, oxidation

1. INTRODUCTION

High energy observatories often require optical and infrared blocking filters to reduce both spurious counts from out-of-band photons and thermal load on the detector. Since these are *transmission* filters, they must be extremely thin freestanding films to maintain high transmission in the soft x-ray bandpass, where all materials are strongly absorbing. The best broadband solution for in- and out-of-band transmission as well as launch survivability is aluminum, while polyimide provides both mechanical strength and UV rejection in a composite filter. Al/LUXFilm®† polyimide filters have a long flight heritage, dating back to the Chandra X-ray Observatory. Typical thicknesses of astrophysical optical blocking filters are 30 nm to 100 nm Al and 50 nm to 150 nm polyimide, with precise specifications depending on bandpass, filter size, and expected mechanical stresses during launch. One path to improved effective area is through filters with higher transmission, and the proposed design for the Lynx x-ray mission [1] decreases those thicknesses by a factor of several while increasing the filter apertures over flight-proven designs (see Fig. 1), pushing the limits of existing filter fabrication technologies.

Of the three primary instruments on Lynx, the Lynx X-ray Microcalorimeter (LXM) [2] presents the greatest challenges from a filter standpoint because it spreads optical blocking across five filters, possibly needing films as thin as 10 nm Al and 20 nm polyimide [3]. Larger and thinner filters increase difficulty of manufacture and decrease mechanical strength – and at 20 nm thickness, the design might push the limits of the molecular structure of LUXFilm®† polyimide. The larger filter area can also increase the need for blocking of out-of-band power.

Physical vapor deposition (PVD) techniques have been the standard for fabricating the metal layers of optical blocking filters since the 1970s [4]. The large-area ultrathin filters of the Lynx design present two fabrication challenges to PVD processes:

1) areal uniformity due to path length differences from the deposition source to disparate regions across a large filter, and
2) formation of islands due to nm-scale growth patterns during deposition [5].

The former can be solved with motion during deposition to change the relative position of the source and filter/substrate, but the entire deposition of a 10 nm to 15 nm film takes under a minute, leaving little time for uniformity through motion.

---

* ben.zeiger@luxel.com | +1 (360) 378-4137 | www.luxel.com
† Trade names are used for completeness. Use of brand names does not constitute endorsement by NIST or the Federal Government

The latter – insular growth in the early stages of film deposition – defines a practical lower limit of deposition for an optical blocking filter. The consequence of thicknesses in this range is the persistence of capacitive islands [6] that behave as low pass filters [7]; above this threshold, the deposition layer grows into a continuous film.

To determine if the Al component of Lynx optical blocking filters is viable with established fabrication techniques, the first prong of this study looks at the uniformity of PVD-manufactured Al filters on large scales through the lens of optical density. The second prong looks at the consequences of thickness on filter lifetimes, since extended Lynx mission plans might eclipse twenty years with exposure to high energy photons and the ion- and radical-rich environment of space. Given two films differing only in thickness, optical properties of the thinner one will be more affected by surface oxidation or other chemical changes.

Aluminum oxidizes readily in air, and Al_2O_3 relative to Al has a much higher visible transmittance and a much lower x-ray transmittance. While Al in standard laboratory environments passivates with a stable Al_2O_3 layer of order 3 nm [8], this might not be the case in high energy observatories. Ultrathin filters in high energy solar observatories have shown significant changes in soft x-ray, EUV, and visible transmittance over their lifetimes [9]. High solar flux is capable of increasing the thickness of the passivating oxide layer on thin metal films, a phenomenon that has also been observed in high-energy synchrotron beamlines. While oxidation has not been observed in thin filters on Chandra and XMM-Newton, Lynx, and LXM in particular, presents new challenges: filters are much thinner, so a thin passivation layer represents a larger fraction of the filter; focal plane cryogenic requirements are more stringent; and the dimensions are far larger. Transmission properties of thin films also suffer more significantly from oxidation than those of thicker films because the oxidation layer is a larger fraction of the filter. While oxidation has thus far only been identified as a potential problem in solar instruments the desired 20-year extended mission for Lynx raises the potential for time to make up for the difference in intensity between the sun and distant stars.

The two components of this study are nearly independent components, linked by the filters rather than the method. We look only at the Al component of a filter, since the polymer component – needed for both strength and UV blocking – is partially a mechanical and system-level solution. We examine Al films manufactured with established PVD techniques to evaluate whether they are sufficient to meet Lynx requirements. Sections 2 and 3 contain the method and results of the deposition characterization, while Sections 4 and 5 detail the method and results of the endurance study. Section 6 offers overall conclusions on the state of optical blocking filters as relevant to the Lynx mission, including an outline of where additional effort would be well-spent for filter optimization.

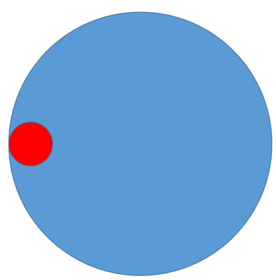

Figure 1. Relative sizes of the Ø1cm Hitomi (small) and Ø6cm extended Lynx (large) microcalorimeter focal plane arrays in need of optical blocking filters.

1.1 Lynx X-ray Microcalorimeter

The LXM will employ at least five filters to separate the several stages of the cryostat. Early Lynx requirements set high throughput at 200 eV as a significant requirement, although this has become less of a science driver recently [10]. The in-band transmittance requirements will be set by science goals, while the out-of-band rejection specification is a combination of cryogenic capabilities and detector capabilities. As an example of requirements for the sake of comparison, the transmittance requirements for the Hitomi microcalorimeter filter stack are listed in Table 1.

Transmission and strength requirements dictate filter materials. The transmittance of a 200 nm thick Al film is about 0.6 at both 21 and 41 eV, but only 120 nm of Al is needed to meet the infrared transmission specifications. Polyimide, on the other hand, is transparent in the IR but is highly absorptive in the UV, and a 200 nm thick LUXFilm®† polyimide film transmits 2.9×10^{-7} at 21.2 eV and 7×10^{-3} at 42.8 eV [11]. Both Al and polyimide are effective blocking filters at 10.2 eV, where a single 20 nm Al/50 nm LUXFilm®† polyimide filter would meet the $<2\times10^{-3}$ transmittance specification. Athena designs are considering 45 nm polyimide/30 nm Al filters throughout the cryostat filter stack [12], while Hitomi used at least 75 nm LUXFilm®† polyimide on each cryostat filter [13].

This study does not address freestanding Al (no polyimide), although this is used in some terrestrial microcalorimeter optics. At the thicknesses desired for Lynx, a 6 cm diameter aperture would require a mesh support to withstand launch. The mesh component makes this a significant engineering undertaking, and one too large for the scope of this study. At present, mechanical requirements for a freestanding Al filter would require a thickness much greater than 50 nm. Similarly, we have not addressed optimization of the polyimide thickness because of its role in mechanical support.

Table 1. Transmittance requirements for the Hitomi microcalorimeter filter stack [12].

Energy	Transmittance
10 keV	>0.70
6 keV	>0.70
1 keV	>0.52
0.6 keV	>0.16
40.8 eV	<0.006
21.2 eV	<0.02
10.2 eV	<0.002
0.040-0.40 eV	$<5\times10^{-9}$

1.2 HDXI and XGS

The other instruments on Lynx – the High-Definition X-ray Imager (HDXI) [14] and X-ray Grating Spectrograph (XGS) [15, 16, 17] – are much less of a challenge from an Al deposition standpoint, although the large aperture of the HDXI presents mechanical challenges. The baseline of a 30 nm Al optical blocking filter, either directly deposited onto the detector or onto a polymer filter (for UV absorption and better optical blocking) is within the current limits of deposition technology. It may be desirable to deposit the 30 nm Al in two 15 nm layers to reduce pinhole density. In that case the thickness is in the realm of this study.

Both the Lynx HDXI and XGS teams have expressed an interest to minimize absorption of the 277-eV carbon line. However, polyimides have a high carbon density, which could be a problem if the carbon line is shifted to higher energies. We acquired several ~10 cm^2 samples of 20 nm Si_3N_4, and this thickness has been manufactured at Lynx scales (>10 cm×10 cm) for use in other industries. Depositing onto such a thin film can present challenges due to heating, chemical stresses, and damage to the film by deposition of hot particles. We coated several of these samples with 30 nm Al to establish the viability of this method to see if the membranes would create a comparable Al structure to that seen on polyimide.

Polyimide versus silicon nitride considering the C line is a decision that will rest heavily on science requirements: specifically, whether the driving scientific interest is in the local universe or the highly redshifted one. (There is a mechanical trade to be considered between polyimide and Si_3N_4 as well.) The transmittance of polyimide per unit thickness at energies less than 277 eV is decidedly better than that of Si_3N_4, (Fig. 2) largely because of the significant density difference between the materials.

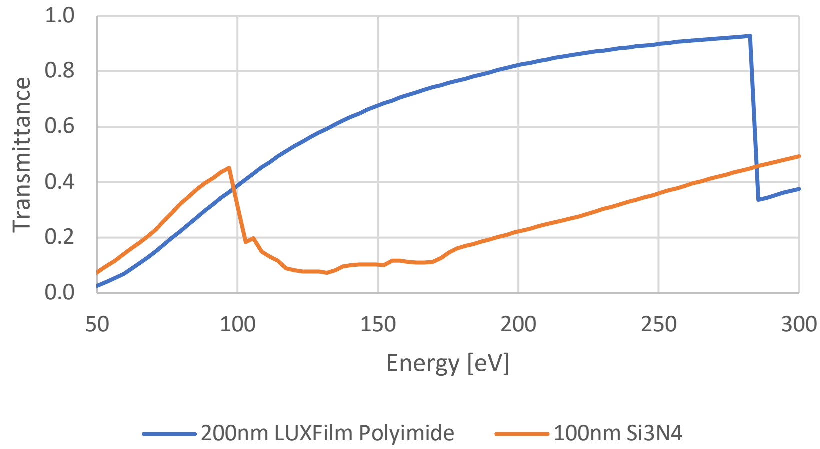

Figure 2. Modeled transmittance of 100nm Si_3N_4 and 200nm LUXFilm®† Polyimide® filters. Polyimide density is 40% that of Si_3N_4. Source: http://henke.lbl.gov/optical_constants/filter2.html [11]

2. DEPOSITION STUDY METHOD

2.1 Filter Materials

We used an electron beam deposition source in a ~10^{-9} bar vacuum to deposit 15 nm to 20nm Al films onto LUXFilm®† polyimide, with Al coatings in the 10 nm to 20 nm range. These filters were divided into 1 cm apertures for testing in our benchtop spectrometers and imaging photometer (Section 3) to look at optical and infrared transmittance as a function of position across a single large filter and as a function of thickness to see how thin we could deposit a viable Al layer for a Lynx filter degradation of optical blocking due to a discontinuous film.

We performed the same tests on filters from old Luxel orders with 15 nm to 45 nm Al thickness to increase the statistical scope of this study. We also looked at two alternate solutions: increasing the number of Al surfaces by depositing on both sides of the polyimide (spacing the two Al layers by much less than the micron-scale wavelengths of interest) and using a 5 nm amorphous C layer as an intermediate to increase the density of nucleation sites and reduce island growth.

2.2 Characterization Methods

The following instruments were used for characterization of Al deposition:

1. KLA P-7†: Stylus profilometer used for measuring the thickness of Al and polyimide witness samples produced alongside the studied filters. Thickness uncertainty is ±1.5nm.
2. Transmission Imaging Photometer (TIP): A custom-built photometer for measuring broadband visible transmission through filters. It backlights filters with a tungsten-halogen bulb, and a high-sensitivity camera captures transmittance with spatial resolution of ~60 µm. The instrument has a bandpass of 400 nm to 700 nm and a lower transmittance limit of ~10^{-9}. This is part of Luxel's standard outgoing inspection of filters, giving an extensive data set to which to compare results.
3. Thermo Evolution 60s†: Ultraviolet/visible (UV/Vis) spectrometer with a 190 nm to 1100 nm bandpass. The lower transmittance limit is 10^{-4}.
4. Nicolet iS10†: FTIR spectrometer with a 1-25 µm bandpass. Its lower transmittance limit is ~10^{-6} out to ~10 µm. The iS10 has NIST-traceable internal calibration standards.

3. DEPOSITION STUDY RESULTS

We measured 45 films in total, spanning 18 aluminum deposition runs.[1] Data for select wavelengths are shown in Fig. 3, translated to attenuation coefficients by dividing the logarithm of transmittance T by film thickness z:

$$\alpha = -\ln(T)/z \qquad (1)$$

Data at wavelengths ≥3 µm are more reliable than those at shorter wavelengths, as small transmittance peaks in the visible and near IR shift slightly with thickness, so transmission at a fixed wavelength can be misleading. Since soft x-ray attenuation coefficients are slowly varying in the bandpass of a filter, the visible and infrared attenuation coefficients are a reasonable figure of merit in filter design to maximize in-band and minimize out-of-band transmittance. Figure 3 includes surface reflection in its attenuation coefficient, so thinner continuous films would be expected to have larger values of α. However, the slope of α appears to decrease below about 20 nm to 25 nm, indicating this to be the lowest Al thickness providing continuous coverage.

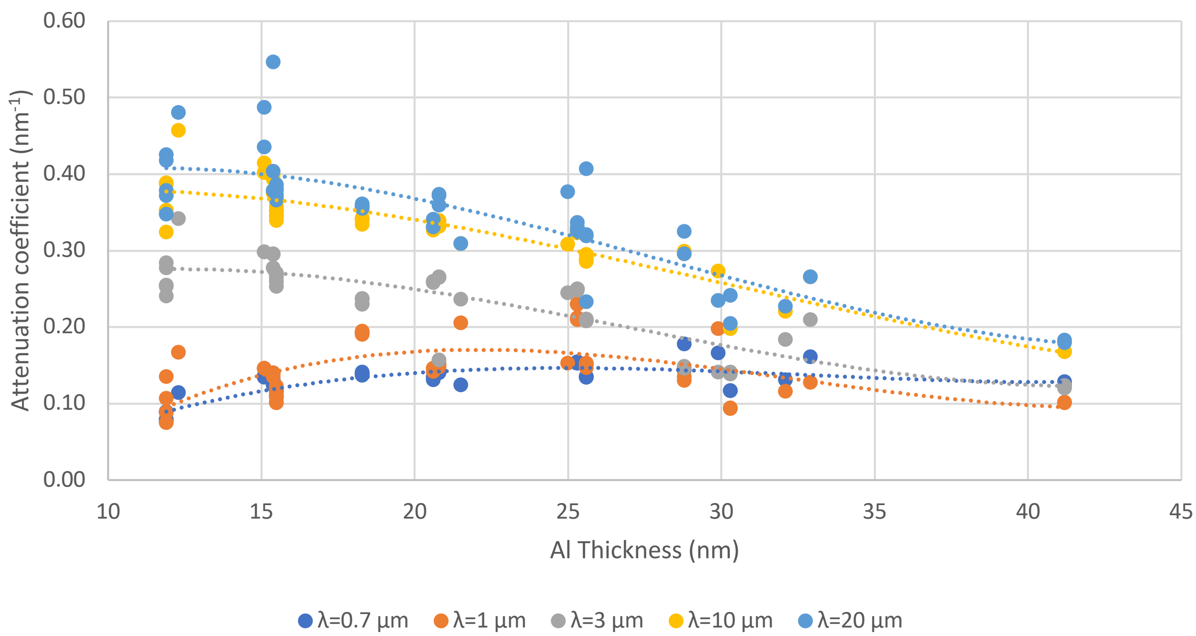

Figure 3. Attenuation coefficient as a function of aluminum thickness, measured at five different wavelengths for 45 films. Data at 12.3 nm have a 5 nm C layer contributing to attenuation, while points at 30.3 nm and 41.2 nm are through two Al layers split evenly on either side of a polyimide film. Attenuation coefficients are calculated with Eq. 1 without accounting for reflectance. Dotted lines show general trends via 3rd order polynomials from empirical fits, not theoretical models; data for wavelengths ≥3 µm show increased attenuation per unit thickness even at 11 nm, indicating that these thicknesses have enough surface reflection at long wavelengths that they are potentially useful deep in a cryostat where IR transmission is the primary concern.

By 40 nm thickness, Al is continuous and sufficiently thick that the film behaves as a "thick" Al filter, at least from an optical perspective. Our historical measurements with our Transmission Imaging Photometer give an attenuation coefficient of Al of 0.14 nm^{-1} to 0.15 nm^{-1} in the visible for Al films <150 nm thick.

[1] Aside from several absorption lines, polyimide is nearly transparent in the infrared and was treated as insignificant. At thicknesses up to 500 nm, the polyimide transmittance is >0.8; varying thicknesses in inventoried material can account for only a small portion of the 0.7µm and 1.0µm variability.

Data aligned vertically in Fig. 3 is from the same deposition run and taken from various locations within a roughly 10 cm diameter to explore uniformity across the deposition run. Attenuation coefficients are generally grouped within about 10 %, with slow variations across the filter.

Figure 3 includes three experimental filters described in Section 2.1:

- Data at 30.3 nm and 41.2 nm Al are from films with nearly equal thicknesses split on two faces of 45 nm polyimide. As the separation is much less than a wavelength, we did not expect to see a repeat surface reflection, and the optical attenuation is, if anything, worse than single-layer Al of equivalent thickness.
- Data at an Al thickness of 12.3 nm includes a 5 nm C layer to change Al growth structures. This decidedly increased the attenuation coefficient, suggesting that the intermediate C layer might provide a better substrate than bare polyimide for ultrathin Al. Statistics here are quite low, however, and we have not attempted to remove the (small) attenuation due to C from the transmission profile. Despite being a better film from the standpoint of optical attenuation, the polyimide/C/Al film was very fragile and could only be tested on a several-mm aperture.

We also investigated uniformity across large spatial scales by taking samples across four 130 mm diameter deposition substrates, comparable to a full LXM filter. Measurements are shown in Fig. Figure **4**, with 18.3 nm and 25.3 nm Al films showing good uniformity through the infrared, while the 11.9 nm Al film is notably worse than the other three.

Al with a thickness <15 nm on 45 nm to 50 nm polyimide is quite difficult to work with generally, and we only produced filters this thin up to 3 cm in diameter for this study. Working with 20 nm Si_3N_4 was even more challenging, as the filters

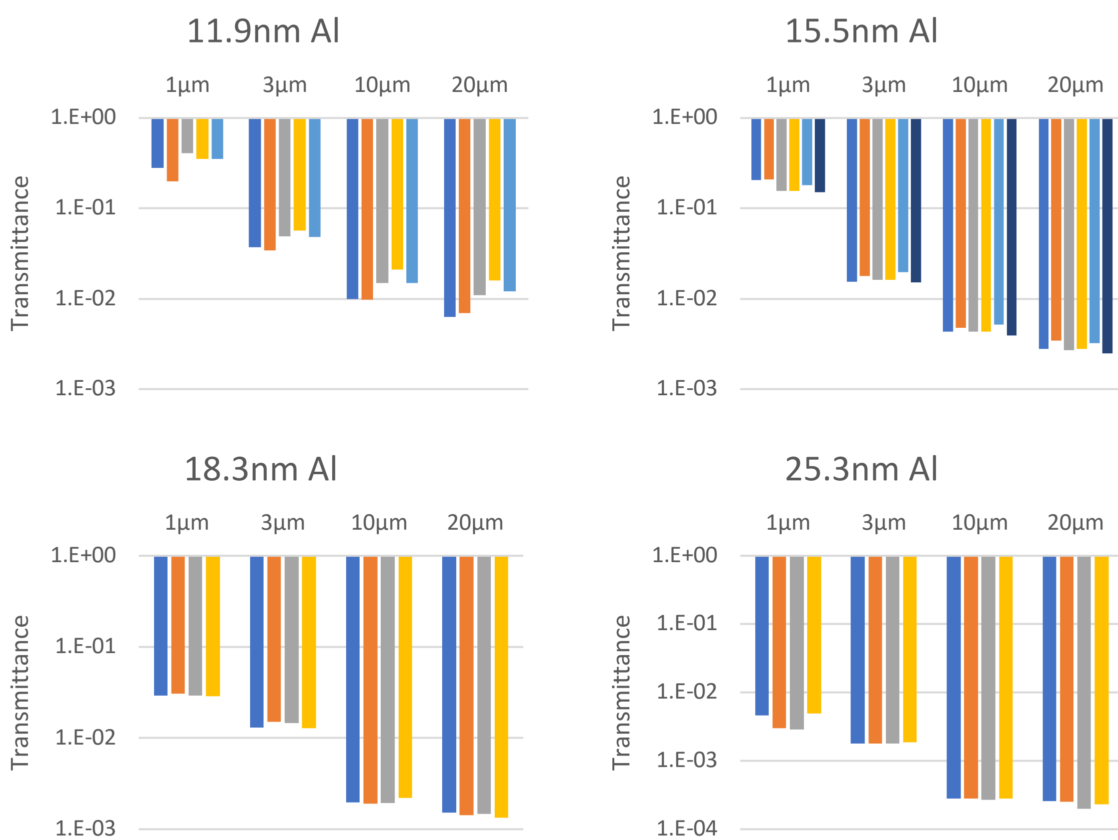

Figure 4. Transmission measurements made at several locations around four 130 mm diameter filters of different thicknesses, with the different colors indicating different positions. All depositions were made onto 50 nm LUXFilm®† polyimide; each bar graph is labeled with the Al thickness and shows transmission at four wavelengths.

are highly sensitive to air currents and static charges. We were able to measure one 30 nm Al deposition on a Si_3N_4 membrane with our imaging photometer, seeing an optical density around 0.85 that of a 30 nm Al deposition on polyimide. The film was quite fragile, and we were not able to measure it on our spectrometers.

4. ENDURANCE STUDY METHODS

Thin Al/polyimide filters underwent accelerated aging tests on Beamline 1 [ref. 18] of the NIST Synchrotron Ultraviolet Radiation Facility (SURF III) storage ring [19]. Briefly, this beamline consists of a single Mo/Si spherical multilayer mirror, which collects and focuses broadband radiation from SURF III. A fused silica window limited the band pass to wavelengths longer than 170 nm, while the synchrotron radiance weighted the spectrum so that most of the beam energy was near the window cutoff. The peak irradiance is about 3 mW mm^{-2} in the wavelength region of interest. Test conditions varied VUV dose and water vapor partial pressure, as described in Table 2. Water pressure was measured with an ionization gauge. The absolute pressure uncertainty is 50 %, but the gauge is linear to a few percent. The incident power was measured with a NIST-calibrated photodiode, and the total dose has an uncertainty of 5 %. The spot size was such that 50 % of the radiation fell in a spot 0.64 mm × 1 mm. Four spots were exposed to different conditions on each of three filters (see Fig. 5). The relative transmission of the incident radiation was measured every 30 min during exposure with a photodiode.

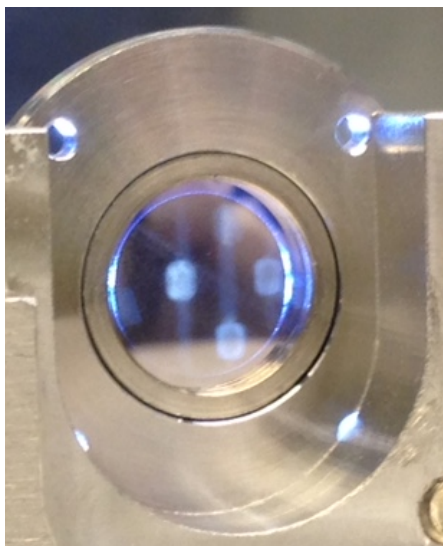

Figure 5. Backlit image of TF110-2186 after exposure to the SURF III beamline in four locations. The top spot was exposed to UV photons in a dry vacuum, while the other three were exposed to varying UV doses after the introduction of 1.3×10^{-6} mbar H_2O vapor. TF110-2186 was irreparably damaged before the oxidation could be quantified.

After exposure, films were evaluated with transmittance scans at 17.5 nm and 532 nm wavelengths with 100 µm spatial resolution at SURF Beamline 7. Oxidation of filter TF110-2189 was directly measured with x-ray photoelectron spectroscopy (XPS). TF110-2187 thickness was measured at Luxel via optical modeling of visible reflectance spectra (380 nm to 1000 nm using a Filmetrics† F10-AR reflectometer) to determine the extent of polyimide degradation.

Table 2. Filter test conditions.

Filter	Material	Exposure conditions (water vapor pressure, VUV dose)
TF110-2186	46.3 nm polyimide, 20.8 nm Al	60 J no water vapor; 60 J, 150 J, and 200 J with 1.3×10^{-6} mbar H_2O pressure
TF110-2187	46.3 nm polyimide, 20.8 nm Al	150 J; 1.3×10^{-5} mbar, 4×10^{-6} mbar, 4×10^{-7} mbar, and 1.3×10^{-7} mbar H_2O pressure
TF110-2189	54.3 nm polyimide, 16.4 nm Al	1.3×10^{-6} mbar H_2O pressure; 130 J, 205 J, 500 J, 1500 J

5. ENDURANCE STUDY RESULTS

Films showed a sharp initial rise in UV transmittance during exposure, as shown in Fig. 8. Visible transmittance measured at the end of exposure (Fig. 6, as optical depth at 532 nm wavelength) also increases in the exposed regions of the film. The 50 nm thick polyimide is nearly transparent at a wavelength of 532 nm, and the decrease in optical depth is, therefore, due to oxidation of Al rather than to ablation of polyimide.

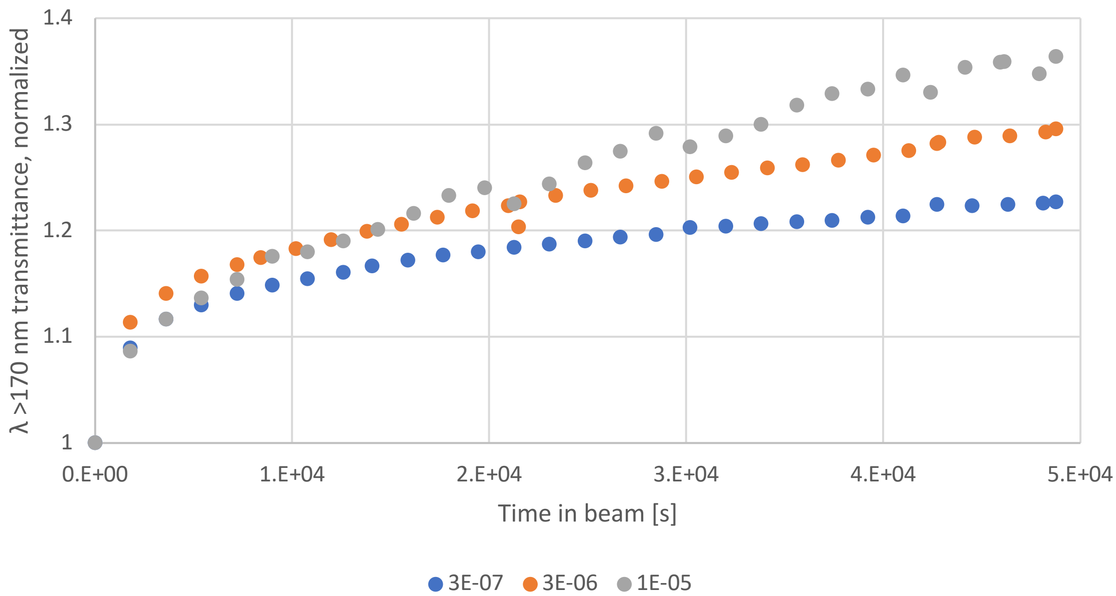

Figure 6. Transmittance of TF110-2187 as a function of time in beam for three different H_2O partial pressures. By first measurement at 1800 s, transmittance in all three spots had increased by ~10%. The 1800 s cadence corresponds to 5.4 J; the total dose for each run was 150 J. The later ($>2\times10^4$ s) linear slope is 5×10^{-4}, 9×10^{-4}, and 10^{-3} J^{-1} respectively from low to high pressures. As noted in the text, most of the energy is near the λ>170 nm window cutoff.

Optical measurements at 532 nm show a decrease in optical depth due to Al oxidation at the center of the beam (Fig. 7). Measurements at a wavelength of 17.5 nm show a more complicated profile (Fig. 8). Polyimide is transparent at a wavelength of 532 nm, but its transmittance is much lower at 17.5 nm. A two-peaked profile indicates both oxidation (the negative profile, where increased oxidation reduces transmittance) and polyimide ablation (the positive profile, where decreased polyimide absorptance results in higher transmission). This interpretation is confirmed by reflectometer measurements of polyimide thickness on an exposed spot (Fig. 9).

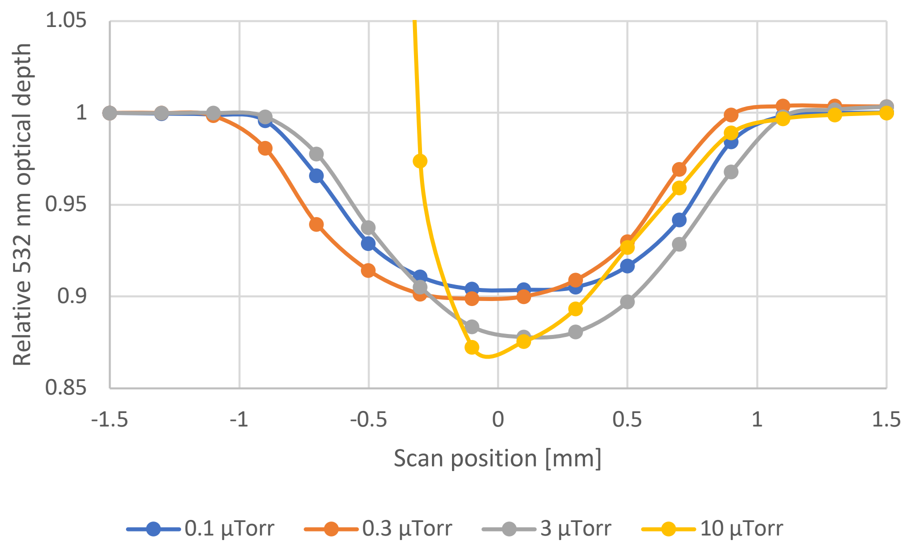

Figure 8. TF110-2187 relative 532 nm optical depth (ln(transmission at location)/ln(transmission of unexposed film)) of exposed spots at varying H_2O pressures and 150 J dose. The 1.3×10^{-5} mbar spot was too close to the edge for a full scan.

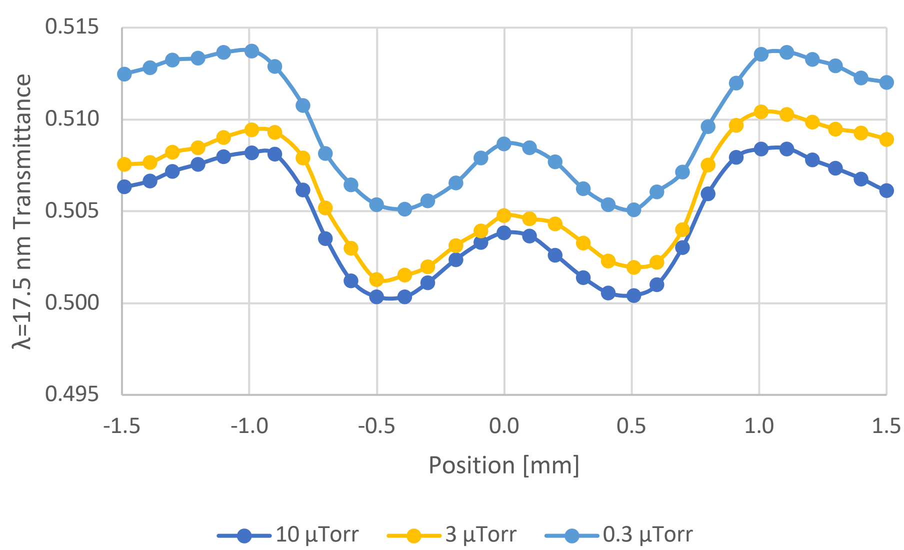

Figure 7. TF110-2187 transmittance at a wavelength of 17.5nm after VUV exposure at varying water partial pressures. Profiles appear to be overlaid features, with a narrow positive feature and a wider negative one.

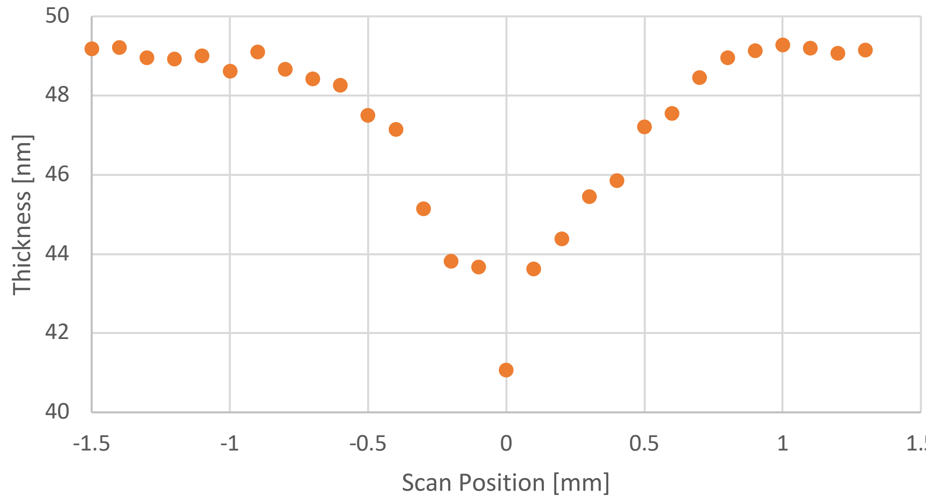

Figure 10. Post-exposure optical reflectometer measurement of LUXFilm® polyimide thickness of TF110-2187. The anomalous point at 0 mm is likely a bad measurement. Optical thickness measurements require a model based on optical constants that might change in an ablated film, so the magnitude of the decrement should be taken as approximate at best. The discrepancy between the nominal thickness in Table 2 and the reflectometer thickness are due to optical modeling accuracy.

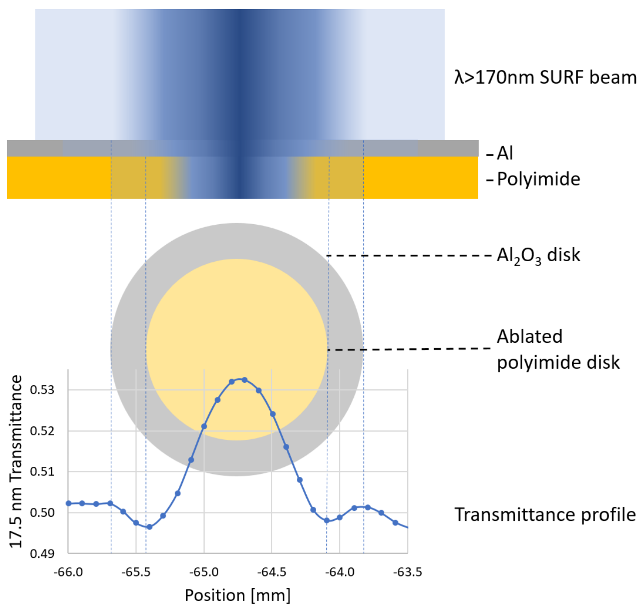

Figure 9. λ=17.5nm transmittance of the 1500 J spot on TF110-2189, with a crude model of SURF beam (blue, top; wavelength > 170 nm), attenuation in the Al layer (gray, top), and a smaller ablation spot in the polyimide as detected with 17.5 nm transmittance and optical reflectometry.

3.0 nm, 3.3 nm, and 3.7 nm for a dose of 150 J and H_2O pressures of 1.3×10^{-5} mbar, 4×10^{-6} mbar, 0.4×10^{-5} mbar, and 1.3×10^{-7} mbar. The exposure increased the oxide layer by about 1 nm.

The data in Fig. 6 can be explained as two processes at work. The initial 2 % J^{-1} rise can be attributed to rapid oxidation of the Al film, which slow as the oxide layer, which serves as a barrier, grows thicker. The later linear rise is primarily due to the continuous ablation of the polyimide film (note that Fig. 6 plots transmittance, not thickness), which presents a nearly-constant thickness (only 10 % reduction) to a nearly-constant beam (10 % increase through the oxidized Al film). The spatial distributions of the oxidation of Al and ablation of polyimide appear to be different, as shown in Fig. 10.

The polyimide ablation rate appears dependent on the square root of the H_2O pressure, which is consistent with the known susceptibility of polyimide to oxygen plasmas [20]. This implies that the oxygen in the presence of the UV beam is to blame for ablation, and degradation is not driven primarily by the UV beam alone.

Also, because the dose is delivered in a range where polyimide and aluminum both have high absorptivity, we cannot disentangle the dose to the polyimide from the dose to the aluminum. However, as these filters mimic the probable Lynx design, we can use it for analysis of the general photon radiation tolerance.

The most relevant question before attempting to disentangle the two is whether this degradation rate matters at all for astronomical filters. The high doses of these tests present a sort of worst-case scenario: if oxidation is negligible, then oxidation is almost certainly not a concern for this mission. On the other hand, if oxidation is not negligible, then this should be studied with test conditions that emulate more accurately the expected operating environment.

The broadband flux (not just UV and higher energies, which are probably most relevant to oxidation rate) from Sirius (to take a bright UV source) would be $\sim10^{-7}$ W m^{-2}, so a 2 m^2 collecting area and a 20 yr life spent 100 % on-source gives 130 J spread across a ~30 cm^2 filter. The spots on TF-2187 were exposed to a total dose of 150 J, which over the central region of the spot gives a total dose of about 150 J mm^{-2}, or about 4.5×10^5 J across a 30 cm^2 filter. TF110-2187 shows a 10 % increase in visible transmittance and a 3 nm to 5 nm decrease in polyimide thickness for a dose of 150 J. Enduring a dose more than three orders of magnitude over that of a bright astronomical source indicates that **photon-driven oxidation of Al and polyimide degradation is not a concern for Lynx filters**, or for any non-solar mission on the horizon.

This study identifies polyimide ablation as a possible concern for Sun-facing instruments, especially in an oxygenated environment such as low Earth orbit. Polyimide degradation at L2 due to an astronomical telescope beam is not a concern.

6. CONCLUSIONS

6.1 Deposition Study

From an Al deposition standpoint, filters do not appear to be a hurdle for Lynx as currently designed. Large-scale uniformity is good, with variations of <10 % across Lynx-scale filters. In Luxel's experience, the variability drops tremendously with thicker films, and Al films with thicknesses >50 nm that have flown on previous missions differed in thickness by less than a few percent across similar apertures. Spectra suggest that, with Luxel's current processes, the Al films are no longer continuous at an Al thickness <15 nm. While this is not a problem optically, telescopes in environments with significant atomic oxygen would see degradation of polyimide in such a thin filter [21].

Technology development efforts for the Athena mission have already demonstrated slightly thicker filters of appropriate lateral dimensions, with 30nm Al supported by 45nm LUXFilm®† polyimide and a mesh with 5mm pitch at a diameter of 100mm [22]. Considerable gains could be made in the quality of Al films in the 10 nm thickness range, although this study demonstrates the viability of filters made with existing production methods, especially beneath the outer filter of a cryostat where the filter will not see ions or radicals. For improving aluminum deposition, possible routes could include surface treatment of the polyimide, reduced substrate temperatures to reduce atom mobility during deposition, and deposition surface energy modification via alloying.

This study did not look closely at the mechanical aspect of thin Al/polyimide filters. Reaching the 20 nm polyimide thickness under consideration will take considerable effort for support meshes and polymer development. Silicon nitride films offer promise, and it is difficult to resist the mechanically integrated beauty of Al deposited onto a membrane and the Si wafer selectively etched to leave a supporting mesh. It also has demonstrated production at 10 nm over small apertures. However, Si_3N_4 has much less heritage for launch and survival in space environments and needs significant development to be viable for large area filters.

6.2 Endurance Study

Results demonstrate that photon-driven Al oxidation and polyimide ablation are unlikely to be problems for the extended Lynx mission, even when using 15 nm Al surfaces. Damage from prolonged exposure to atomic oxygen is still a possible concern if the Lynx orbit shifts to one where oxygen density is higher, while micrometeorites present the bigger threat at L2.

6.3 Path Forward for Lynx Filters

Aluminum and polyimide composite optical blocking filters have twenty years of flight heritage, but large missions such as Lynx require custom form factors. Since thickness and aperture change both optical and mechanical properties, filters for every new mission restart the NASA Technology Readiness Level (TRL) ladder at 5 or lower. This study shows that the Al component of optical blocking filters for Lynx is at TRL 5, with a demonstration of performance in a relevant laboratory environment. TRL 6 requires form, fit, and function to be met in a relevant environment, and thus it invokes mechanical challenges that were not addressed herein. Filter fabrication and survival statistics should be revisited as the Lynx system requirements are better defined (e.g., detector size; transmission requirements; orbit).

This study demonstrates that current technologies are adequate to create a filter that meets the current optical blocking and lifetime requirements for the Lynx mission, but it does not address optimization for a design. Optical blocking filters are the biggest loss of effective area at energies below 500 eV in most soft x-ray telescopes, and they represent a path where large gains can be made through optimization. If the optimization path leads to non-standard methods of filter production, the TRL will drop accordingly. This effort should begin as early as possible and with the attention afforded to other mission-critical components.

Optimization parameters will depend on detector and cryogenic factors, as well as mechanical loading during launch. If the optical blocking requirements point toward an Al thickness requirement <15 nm, more out-of-the-box solutions to change growth patterns (e.g., with an initial monolayer of Al or Al_2O_3 or a light-element intermediate layer similar to the C layer used in this study) would be worth deeper investigation to improve optical density with a minimal increase of x-ray attenuation. If the requirements are for thicknesses >20 nm, then existing processes suffice.

The bigger gains in filters will come from mechanical optimization, where Al plays only a small role. Once the filter aperture is defined, support structure, polyimide thickness, and launch vibrations will determine survival statistics. Overbuilding a filter is different than overbuilding a typical mechanical structure: although Lynx cannot afford to have a filter fail on launch, the converse – sacrificing twenty years of performance to survive several minutes of launch – is also unappealing. Finding the middle ground should be the primary focus of filter development as Lynx development moves forward, although again, this is optimizing standard processes and it should not be seen as a major hurdle.

The potential science return of removing C from the HDXI optical blocking filter (e.g., a Si_3N_4 membrane instead of polyimide or direct deposition of Al onto the detector) is potentially significant, while alternatives to simple thickness optimization, such as laminates, alternate mesh materials and geometries (e.g., Hitomi's hierarchical Si mesh [13]), and better thermal control of filters could each contribute significant improvements in effective area. These improvements will benefit any mission and are worthy of consideration without waiting for adoption of Lynx, although they need significant improvements to rival Al/polyimide filters for optical blocking.

Alternative filter designs such as waveguide-cutoff filters – meshes with sub-wavelength apertures – can offer significant advantages deep in a cryostat, where Al/polyimide filters on warm stages have already attenuated the visible and ultraviolet spectrum. For the innermost filters, the primary concern is blocking the long wavelength infrared radiation from the warmer stages, so these filters can have open (100% transmissive) apertures of several microns.

Acknowledgments

The endurance study relied heavily on Thomas Lucatorto, Robert Berg, and Shannon Hill (now at KLA) at the National Institute of Standards and Technology and Andrew Jones at the Laboratory for Atmospheric and Space Physics for beamline exposures, both transmittance and XPS analysis, and conversations about the significance of results.

Megan Eckart (NASA) provided valuable insights about requirements and paths for future filter development.

This work was funded through cooperative agreement 80MSFC17M0017 between NASA-Marshall Space Flight Center and Luxel Corporation.

REFERENCES

[1] Gaskin, J. et al. “Lynx x-ray observatory: an overview,” J. Astron. Telesc. Instrum. Syst. 5(2), 021001 (2019).

[2] Bandler, S. et al., "Lynx x-ray microcalorimeter," J. Astron. Telesc. Instrum. Syst. 5(2), 021017 (2019).

[3] Eckart, M. E., Yoon, W., Zeiger, B., Bandler, S. R., and McCammon, D, "Design of optical/IR blocking filters for the Lynx X-ray Microcalorimeter," J. Astron. Telesc. Instrum. Syst. 5(2), 021020 (2019).

[4] Steele, G. N., "Development and Fabrication of Large-Area Extreme-Ultraviolet Filters for the Apollo Telescope Mount," Space Optics, Proceedings of the 9th International Congress of the International Commission for Optics, 367. Santa Monica, Ca: National Academy of Sciences (1974).

[5] Petrov, I., "Microstructural evolution during film growth," J. Vac. Sci. Tech. A21, S117-S128 (2003).

[6] Carrio, A. C. "Ultra-thin silver based infrared solar filter for opthalmic lenses," Escola Tecnica Superior d'Enginyeria de Telecomunicacio de Barcelona (2011).

[7] Peng, Y., Paudel, T., Chen, W. C., Padilla, W. J., Ren, Z. F., & Kempa, K., "Percolation and polaritonic effects in periodic planar nanostructures evolving from holes to islands," Applied Physics Letters, 97(4), 041901 (2010).

[8] Cabrera , N, and Mott, N. F., "Theory of the oxidation of metals, Rep. Prog. Phys 12, 163-184 (1949).

[9] Chkhalo, N. I., et al., "Thin film multilayer filters for solar EUV telescopes," Appl. Opt. 55, 4683-4690 (2016).

[10] Bandler, S., "Lynx Microcalorimeter Specifications & Requirements," 25 January 2018, <https://wwwastro.msfc.nasa.gov/lynx/docs/meetings/F2F04/Lynx_F2F4_Bandler.pdf>

[11] Henke, B.L., Gullikson, E.M., and Davis, J.C., "X-ray interactions: photoabsorption, scattering, transmission, and reflection at E=50-30000 eV, Z=1-92, Atomic Data and Nuclear Data Tables," 54 (2), 181-342 (1993).

[12] Barbera, M., Argan, A., Bozzo, E., Branduardi-Raymont, G., Ciaravella, A., Collura, A., et. al, "Thermal Filters for the ATHENA X-IFU: Ongoing Activities Toward the Conceptual Design," Journal of Low Temperature Physics, 184(3), 706-711 (2016).

[13] Kilbourne, C. A., Adams, J. S., Brekovsky, R. P., Chervenak, J. A., Chiao, M. P., Eckart, M. E., et al, "Design, implementation, and performance of the Astro-H soft x-ray spectrometer aperture assembly and blocking filters," J. Astron. Telesc. Instrum. Syst., 4(1), 011215 (2016).

[14] Falcone, A. D. et al., "The high definition x-ray imager instrument on the Lynx x-ray surveyor," Proc. SPIE 10699, 1069912 (2018).

[15] McEntaffer, R. “Reflection grating concept for the Lynx x-ray grating spectrograph,” J. Astron. Telesc. Instrum. Syst. 5(2), 021002 (2019).

[16] Günther, H. M. and Heilmann, R. K., “Lynx soft x-ray critical-angle transmission grating spectrometer,” J. Astron. Telesc. Instrum. Syst. 5(2), 021003 (2019).

[17] Bautz, M., Lynx Instrument Specifications & Requirements: Part 1. HDXI and XGS. 25 January 2018, <https://wwwastro.msfc.nasa.gov/lynx/docs/meetings/F2F04/Lynx_F2F4_Bautz.pdf>

[18] C. Tarrio and S. Grantham, “A synchrotron beamline for extreme-ultraviolet multilayer mirror endurance testing,” Rev. Sci. Instrum. **76**, 056101-104 (2005).

[19] U. Arp, et al., “SURF III: A flexible synchrotron radiation source for radiometry and research,” Nucl. Inst. Meth. A **649**, 12-14 (2011).

[20] Lavoy, R. et al., "A Study of GOES SXI Entrance Filter Designs and the Potential for On-Orbit Degradation," Proc SPIE 70112F (2008).

[21] Parodi, G., D'Anca, F., Lo Cicero, U., Sciortino, L., Rataj, M., Polak, S., et al, "Structural modelling and mechanical tests supporting the design of the ATHENA X-IFU thermal filters and WFI optical blocking filter," Proc. SPIE, 10699, 106994C (2018).

[22] E. Wollack et al., “Technology development of advanced filter design for the Lynx x-ray microcalorimeter,” in preparation (2019).